

Efficiency and robustness in ant networks of galleries

J. Buhl^{1,a}, J. Gautrais¹, R.V. Solé², P. Kuntz³, S. Valverde², J.L. Deneubourg⁴, and G. Theraulaz¹

¹ Centre de Recherches sur la Cognition Animale, CNRS, Université Paul Sabatier, 118 route de Narbonne, 31062 Toulouse Cedex 4, France

² ICREA-Complex Systems Lab, Universitat Pompeu Fabra, Dr Aiguader 80, 08003 Barcelona, Spain

³ École Polytechnique de l'Université de Nantes, 2 rue de la Houssinière, BP 92208, 44322 Nantes Cedex 03, France

⁴ CENOLI, CP 231, Université Libre de Bruxelles, Boulevard du Triomphe, 1050 Brussels, Belgium

Received 16 July 2004

Published online 26 November 2004 – © EDP Sciences, Società Italiana di Fisica, Springer-Verlag 2004

Abstract. Recent theoretical and empirical studies have focused on the topology of large networks of communication/interactions in biological, social and technological systems. Most of them have been studied in the scope of the small-world and scale-free networks' theory. Here we analyze the characteristics of ant networks of galleries produced in a 2-D experimental setup. These networks are neither small-worlds nor scale-free networks and belong to a particular class of network, i.e. embedded planar graphs emerging from a distributed growth mechanism. We compare the networks of galleries with both minimal spanning trees and greedy triangulations. We show that the networks of galleries have a path system efficiency and robustness to disconnections closer to the one observed in triangulated networks though their cost is closer to the one of a tree. These networks may have been prevented to evolve toward the classes of small-world and scale-free networks because of the strong spatial constraints under which they grow, but they may share with many real networks a similar trend to result from a balance of constraints leading them to achieve both path system efficiency and robustness at low cost.

PACS. 89.75.Fb Structures and organization in complex systems – 89.75.Hc Networks and genealogical trees – 87.23.Ge Dynamics of social systems

1 Introduction

Complex systems are composed by sets of interacting units defining a network. Most networks involve information transfer and are not spatially constrained. The analysis of complex webs from both biology, sociology and technology reveal the presence of small-worlds properties i.e. small paths and high local clustering [1–4]. Moreover, these networks are highly heterogeneous and in most cases their degree distributions $P(k)$ are *scale-free*, i.e. are highly heterogeneous with tail decaying as a power law. More precisely, $P(k)$ is the frequency of nodes having k edges and its distribution is characterized by a general form $P(k) \sim k^{-\gamma} \phi(k/\xi)$ where $\phi(k/\xi)$ introduces a cut-off at some characteristic scale ξ . Three main classes have been defined [5,6]: (a) when ξ is very small, the distribution is single scaled, which would typically correspond to a distribution $P(k) \sim e^{-k/\xi}$. (b) as ξ grows, a power law with a sharp cut-off is obtained, i.e. $P(k) \sim k^{-\gamma} e^{-k/\xi}$. (c) for large enough ξ , the distribution is scale-free, i.e. its tails follow a power-law $P(k) \sim k^{-\gamma}$. The presence of

deviations from the SF behaviour are often related to the presence of costly connections [5,7].

In these nets, the cost associated with the connection process is often equivalent for all pair of nodes, and it is often possible to connect any pair of nodes. However many real networks result from construction processes where spatial constraints are at work. In these types of network, two distant nodes are less likely to be connected due to the distance-dependent cost of links. Moreover, in the case of networks where the nodes and edges have a spatial dimension, many direct connections between distant nodes may be not allowed to occur. This is the case in many network structures constructed by human and animals, such as foraging and/or displacement networks [8–11], where the growth of the network progressively fills the space.

Networks hold an essential place in animal societies since they are a by-product of a collective activity and one of the major organizing factors of social phenomena. One of their most frequent function is to allow the efficient movement and communication of individuals inside the structure. Despite the key role of these networks in sustaining society functions, their large-scale structure is essentially unknown.

^a e-mail: buhl@cict.fr

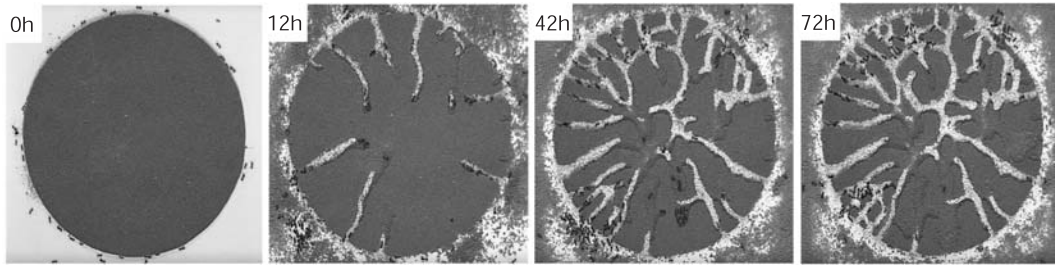


Fig. 1. Example of a gallery pattern produced by 200 ants over 3 days. At the beginning of an experiment, ants are dispersed around the sand disk and can only start to dig it from the periphery. After few hours, several galleries are initiated by group of workers. These galleries stretch inside the sand disk and frequently branch. At the end of the excavation process, after 72 h, a stationary network is obtained and used to generate a static graph.

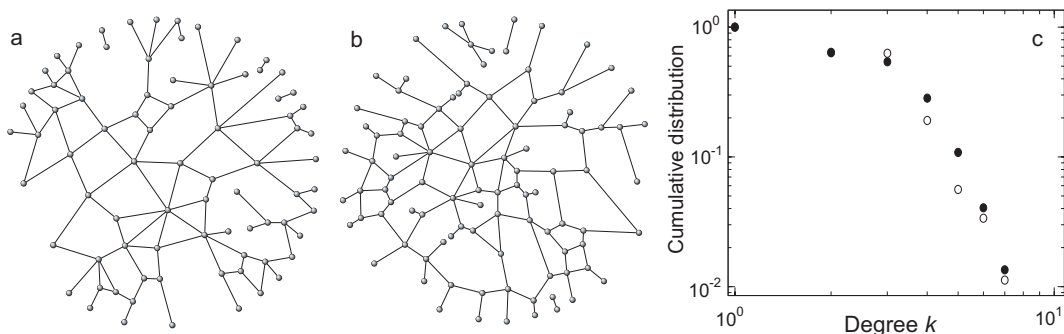


Fig. 2. The graph representation of 2 examples of networks of galleries (a–b) and their cumulative degree distribution (c).

In social insects, nests can be considered as network structures. In ants, a typical underground nest consists in the same basic units: a set of chambers (nodes) interconnected by galleries (edges) [12–20]. The structure of the nests built by different species shows a wide range of variation from non-ramified structures, in the simplest forms, to tree-like shapes and, in the most complex forms, highly connected networks [21]. It can be conjectured that the topological features exhibited by such networks should reflect intrinsic adaptive properties, such as optimal communication and/or robustness against random blocking of given nodes. In this paper we analyze the topological organization of ant galleries as complex networks. Specifically, we study the networks of galleries produced by the ant *Messor sancta* in a two dimensional experimental set-up as an example of emergent organization of network patterns in social insects.

2 Ant galleries as complex networks

The experimental set-up consisted in a sand disk of 20 cm diameter and 5 mm height. We used brusselian sand (a yellow sand of a very fine and homogeneous granularity) that was poured in a mould and humidified by spraying water (25 ml). The mould was then removed and the sand disk covered by a glass plate (25 cm \times 25 cm). An arena ($\varnothing = 50$ cm) with a wall coated with Fluon GP2® was placed around the sand disk to prevent ants from escaping. Each experiment ($N = 19$) began with the random dispersal of 200 ants around the disk. The set-up was videotaped

from above with a high-resolution digital camera and the experiment lasted 3 days. In order to map the network, we used a static snapshot at the end of each experiment. In these conditions, ants are strongly stimulated to initiate galleries that will grow, branch and merge together until achieving a dense network of galleries (Fig. 1). The process reaches a stationary state in which ants do not excavate anymore and the network is completed.

Any of these networks of galleries can be described as an embedded planar graph [22] $G = (V, E)$ where $V = \{(v_i, x_i, y_i), (i = 1, \dots, n)\}$ is the set of n nodes characterized by their (x, y) position, and $E = \{(v_i, v_j)\}$ the set of m edges/connections between nodes and characterized by their length d_{ij} . Edges correspond to subsections of galleries, and nodes to the apices of galleries (dead-ends or openings) or to the intersections between the galleries. These nodes often correspond to simple crossings between galleries but also sometimes to enlarged spaces, namely the chambers, which may contain aggregated individuals, larva, food or refusal material in natural nests [19]. The experimental networks could comprise several connected components. However, the largest connected component always represented the majority of vertices and edges (mean proportion of nodes in the largest connected component: 0.86 ± 0.11). The other connected components were most frequently short abandoned galleries (2 vertices and 1 edge or small trees) which were initiated from the periphery and never merged with other galleries. Since a functional nest in ants is a single connected component, our analysis is restricted to the largest connected component. Examples of these networks are shown in Figure 2.

Table 1. Basic characteristics of the networks: number of nodes n , number of edges m , mean degree $\langle k \rangle$; ξ parameter in an exponential decay $P(k) \sim e^{-k/\xi}$ of the degree distribution tail. Meshedness coefficient M , geometrical and topological global efficiency $E_{glob,G}$ and $E_{glob,T}$ respectively. Robustness to random removal of nodes f_R and selective removal of highest degrees f_S , and relative cost c .

| n° | n | m | $\langle k \rangle$ | ξ | M | $E_{glob,G}$ | $E_{glob,T}$ | f_R | f_S | c |
|-----------|-----|-----|---------------------|-------|-------|--------------|--------------|-------|-------|-------|
| 1 | 88 | 117 | 2.66 | 0.89 | 0.175 | 0.751 | 0.212 | 0.247 | 0.090 | 0.216 |
| 2 | 88 | 114 | 2.59 | 1.02 | 0.158 | 0.662 | 0.226 | 0.286 | 0.102 | 0.206 |
| 3 | 84 | 106 | 2.52 | 0.86 | 0.141 | 0.703 | 0.217 | 0.270 | 0.157 | 0.215 |
| 4 | 74 | 95 | 2.57 | 1.07 | 0.154 | 0.644 | 0.239 | 0.275 | 0.112 | 0.260 |
| 5 | 70 | 84 | 2.40 | 0.69 | 0.111 | 0.496 | 0.230 | 0.224 | 0.059 | 0.143 |
| 6 | 65 | 88 | 2.71 | 1.24 | 0.192 | 0.810 | 0.268 | 0.313 | 0.149 | 0.268 |
| 7 | 62 | 95 | 3.06 | 1.55 | 0.286 | 0.777 | 0.283 | 0.338 | 0.123 | 0.410 |
| 8 | 50 | 60 | 2.40 | 1.01 | 0.116 | 0.559 | 0.256 | 0.246 | 0.131 | 0.171 |
| 9 | 49 | 61 | 2.49 | 1.13 | 0.140 | 0.589 | 0.269 | 0.279 | 0.131 | 0.181 |
| 10 | 44 | 47 | 2.14 | – | 0.048 | 0.570 | 0.254 | 0.231 | 0.096 | 0.079 |
| 11 | 43 | 51 | 2.37 | 1.59 | 0.111 | 0.648 | 0.286 | 0.294 | 0.039 | 0.225 |
| 12 | 42 | 44 | 2.10 | 1.03 | 0.038 | 0.542 | 0.263 | 0.220 | 0.020 | 0.127 |
| 13 | 41 | 51 | 2.49 | 0.95 | 0.143 | 0.573 | 0.287 | 0.274 | 0.078 | 0.190 |
| 14 | 36 | 41 | 2.28 | 0.93 | 0.090 | 0.567 | 0.304 | 0.262 | 0.071 | 0.106 |
| 15 | 36 | 39 | 2.17 | 1.54 | 0.060 | 0.595 | 0.329 | 0.295 | 0.090 | 0.230 |
| 16 | 32 | 37 | 2.31 | 1.07 | 0.102 | 0.510 | 0.327 | 0.289 | 0.089 | 0.181 |
| 17 | 31 | 39 | 2.52 | 0.93 | 0.158 | 0.527 | 0.328 | 0.300 | 0.050 | 0.178 |
| 18 | 23 | 24 | 2.09 | – | 0.049 | 0.471 | 0.366 | 0.312 | 0.093 | 0.067 |
| 19 | 14 | 14 | 2.00 | 1.24 | 0.043 | 0.365 | 0.422 | 0.296 | 0.111 | 0.085 |

Typical measures computed on complex networks involve the average path length L and the local correlations defined through the so called clustering coefficient C [1–4]. For small world nets, L scales as the logarithm of the system size and is close to the random graph distance. This is not the case here, given the spatial constraints. The clustering C is a measure of the fraction of triangles present in the network. However, there exists a whole range of networks which differ in the level of connection between neighbours though their clustering coefficient is always equal to 0: for example, this is the case of markedly different topologies such as a tree, a square and a honeycomb mesh. Indeed, the clustering coefficient is a measure of the structure of cycles restricted to the case of cycles of length 3. It would be thus necessary to find more general measures of the structure of cycles than the clustering coefficient [23]. We define here a *meshedness* coefficient that addresses this question specifically for planar graphs. From the Euler formula, the number of faces (excluding the external one) associated with any planar graph is $f = m - n + 1$. It entails that for such graphs $m \leq 3n - 6$ and consequently the maximal number of faces would be $f_{max} = 2n - 5$. We can thus compute a normalized “meshedness coefficient” $M = f/f_{max}$, where M can vary from zero (tree structure) to one (complete planar graph). This coefficient will be discussed below in relation with efficiency.

An additional global characterization is given by the degree distribution. In contrast with other (large) net-

works such as social, communication or metabolic networks, the constructed networks studied here have a small number of nodes and edges. Moreover, they are planar, which means that, by construction, edges of E intersect on nodes only. Due to these constraints, it is highly unlikely to have a high heterogeneity (i.e. SF distributions). As we can see in Figure 1c, the degree distributions are actually exponential (i.e. single-scaled). Here the cumulative distribution

$$P_{>}(k) = \int_k^{\infty} P(k') dk' \quad (1)$$

is used (see [5]) and shown for three different networks (displayed in a–c). Distribution tails can be approximated by the form $P(k) \sim e^{-k/\xi}$ with ξ ranging from $\xi = 0.69$ to $\xi = 1.59$ (ξ values were determined from the cumulative distributions; Tab. 1).

The standard comparisons with theoretical models (such as the standard, Erdős-Renyi random graph [24]) that were developed in the SW and the SF framework lose their relevance in the context of planar graphs. Unfortunately, there are few general analytic results (such as path lengths or degree distributions) on random planar graphs [25,26]. However, two relevant references can be built from a node set to compare embedded planar networks with. At one extreme, we have tree-like structures, which have been widely used as models of river networks that are obviously spatially-constrained systems [27]. In

particular, the *Minimal Spanning Tree* (MST) defines the shortest tree which connects every nodes into a single connected component [28–30]. At the other extreme, the natural reference should be the *Minimum Weight Triangulation* (MWT) which contains the highest number of edges (with no edge crossings) while minimizing its total length [31]. Yet, no polynomial time algorithm is known to compute the MWT [32]. We thus fell back on the easily computed *Greedy Triangulation* (GT) which connect nodes in the ascending order of edge length provided that no edge crossing is introduced. This leads to a maximal connected graph (still obeying the planar constraint) while minimizing as far as possible the total length of edges [33]. These bounds make also sense as regards the evolution of these networks: the most primitive forms of nest are trees while the most complex forms involve mesh-like patterns [21]. Using the previous definitions and limit models, we will proceed to analyse the efficiency, robustness/fragility and cost of the present ant networks of galleries.

3 Network efficiency

One possible adaptive trend in the architecture of galleries generated by social insects is efficient communication and/or displacements. The characteristics of the path system can be evaluated by the analysis of the shortest-paths between all pair of nodes. Networks of galleries are spatially extended webs, it is thus possible to work with two types of distance metrics: topological and geometrical. The topological measures of the path length corresponds to the number of nodes the path is going through, while the geometrical measure of the path length corresponds to the sum of the distance $d_{i,j}$ of all edges the path is going through. Recently, Latora and Marchiori [34] proposed the so-called “average efficiency”:

$$E(G) = \frac{1}{n(n-1)} \sum_{v_i \neq v_j \in V} \frac{1}{d_{ij}^*}, \quad (2)$$

where d_{ij}^* corresponds to the shortest path between the nodes i and j . For the given graph G , we always compute the efficiency as the ratio between $E(G)$ and $E(K_n)$, where K_n is the complete graph of order n (it possesses the same vertices as G , but with all the $n(n-1)/2$ possible edges). The so-called global efficiency E_{glob} is determined by computing the efficiency measure for all paths in the graph G ,

$$E_{glob} = E(G)/E(K_n). \quad (3)$$

In the networks of galleries, the geometrical efficiency $E_{glob,G}$ varies from $E_{glob,G} = 0.676$ to $E_{glob,G} = 0.812$ but is not correlated with n (Fig. 3a). The values of $E_{glob,G}$ in the corresponding GT networks are always higher than in the networks of galleries, and there is no correlation with the network size n . By contrast, the MST has a rather different behaviour: for small n , $E_{glob,G}$ is similar to what observed in the networks of galleries, but it decreases as a power-law when n increases. The absence

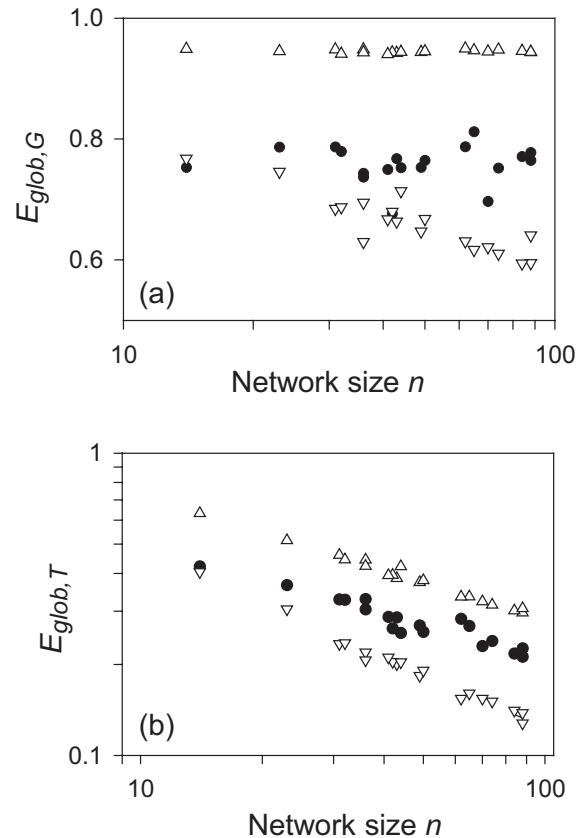


Fig. 3. Relation between geometrical (a), topological (b) global efficiency $E_{glob,G}$ and $E_{glob,T}$ and network size n . $E_{glob,G}$ is independent of n in both the networks of galleries (circles) and the GT networks (upward triangles), while it decreases as a power law in the MST networks (downward triangles). $E_{glob,T}$ decreases with increasing network size n in all networks. However, this decrease is slower in the networks of galleries (circles) than both in the MSTs (downward triangles) and the GT networks (upward triangles).

of decay in $E_{glob,G}$ for the networks of galleries may be related to the presence of a certain degree of meshedness.

In the networks of galleries, the topological efficiency varies from $E_{glob,T} = 0.212$ to $E_{glob,T} = 0.422$ and decreases with n (Fig. 3b). $E_{glob,T}$ also decreases with n in both MSTs and greedy triangulations (Fig. 3b). While this decrease has a similar rate in the latter, the decrease of $E_{glob,T}$ with n in the networks of galleries is clearly slower. For small network size n , it is close to MSTs, but it progressively reaches values closer to a triangulation for higher n . Again, this may be related to an increasing effect of cycles when n increases.

None of the networks of galleries are trees, but the meshedness coefficient M exhibits a certain variability from values close to a tree (minimal $M = 0.038$) to values far from those expected from a triangulation (maximal $M = 0.286$) (Tab. 2). Indeed, M increases with network size n ($r = 0.589$; $N = 19$; $p = 0.008$) and is positively correlated with $E_{glob,G}$ ($r = 0.549$; $N = 19$; $p = 0.015$). The behaviour of geometrical and topological E_{glob} with

network size n may be related to the progressive increase of meshedness of the networks of galleries.

4 Network robustness

Beyond the efficiency associated to a given network topology, an additional and complementary approach is the analysis of fragility against random failures. Such failures might be mutations in gene networks, failures of routers in the Internet or species loss in an ecosystem. The *robustness* of a network can be evaluated by studying how it becomes fragmented as an increasing fraction of nodes is removed. The network fragmentation is usually measured by the fraction of nodes contained by the largest connected component. This node removal can take place either randomly or in decreasing order of their degree (selective removal). In homogeneous random graphs, the fragmentation of the network is similar under random and selective removal of nodes [35,36]. Several real networks have been reported to deviate clearly from this prediction of random graph theory and to exhibit a high resilience to random removal and high vulnerability to selective removal of nodes [35–38]. This property was first proposed as a unique feature of scale-free networks [35]. However several food-webs that are not scale-free networks also exhibit this property, and it has thus been conjectured that it could come from a more general feature of the degree distribution, such as its degree of asymmetry [39] or degree correlations [40]. Here we explore the effects of node removal (here this removal means blocking nodes in the gallery system) and compare them with both MST and GT networks.

For each experiment, we have determined the evolution of the relative size S of the largest connected component, i.e. the fraction of nodes contained in it, with the fraction f of disconnected nodes (1000 runs for each experiment) under a random node removal or a selective removal of nodes in decreasing order of their degree. We define the random and selective *robustness* (f_R and f_s , respectively) as the values of f required for S to reach the value $S = 0.5$ in each type of removal.

The fragmentation curves are similar in all gallery networks analysed (Fig. 4a). The decrease of S is relatively slow when nodes are randomly disconnected, while it is very fast-decaying when higher degrees are disconnected first. This property is very different from what is observed in a classical random graph, where the decrease of S is similar under both random and selective removal of nodes (Fig. 4b).

The specific behavior of fragmentation observed in the networks of galleries may come from a certain level of heterogeneity in the structure of these networks. Indeed there is a significant correlation between f_R and ξ ($r = 0.629$; $N = 17$; $p = 0.005$), indicating that robustness increases with the skewedness of degree distribution, as expected. It is also interesting to note that the random robustness

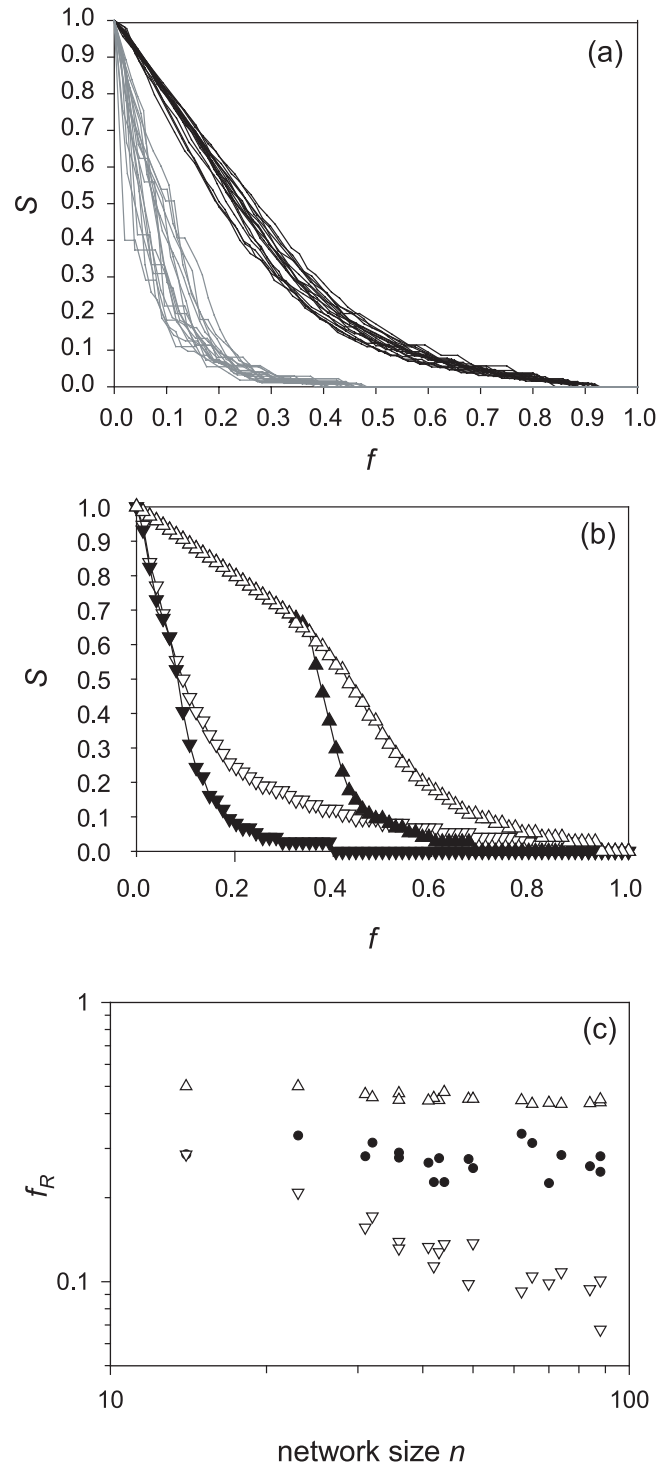


Fig. 4. (a) Galleries' network fragmentation, measured by the relative size of the largest component S , under random (black curves) and selective (grey curves) removal of a fraction of nodes f . (b) Fragmentation of the MST (downward triangles) and GT networks (upward triangles) corresponding to the experiment #4 under random (open symbols) and selective (closed symbols) removal of nodes. (c) Relation between the robustness to random node removal f_R and the network size n . f_R is independent of n both in the GT (upward triangles) and the galleries' networks (circles), while it decreases as a power law in the MST networks (downward triangles).

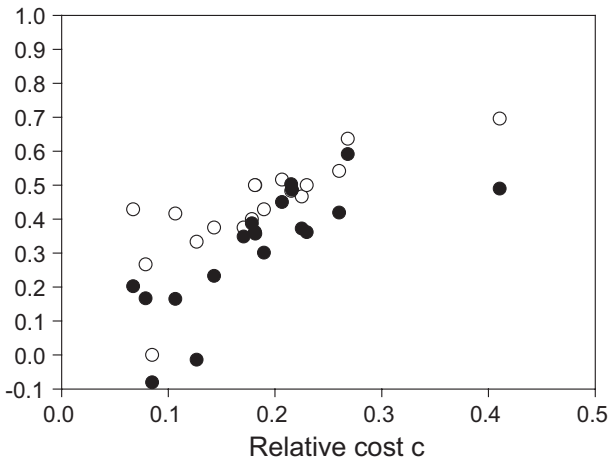


Fig. 5. Relation between relative cost c , relative robustness f_R^* (open circles) and relative geometrical global efficiency $E_{glob,G}^*$ (closed circles). The down-left corner (coordinates 0,0) corresponds to the cost, robustness and efficiency of the MST while the coordinates (1,1) would correspond to these characteristics in a GT network.

is independent of network size n both in the networks of galleries and in greedy triangulations, while it decreases with n in MST (Fig. 4c).

5 Network cost

In the networks of galleries, the counterpart of an increase in E_{glob} and random robustness f_R may be an increase in length, which would also correspond to an increase in the cost of construction. Given a set of n nodes, the shortest network that connects all nodes correspond to the minimal spanning tree, while a maximal cost is met with GT networks. We thus defined a normalized cost measure as

$$c = \frac{L_{EXP} - L_{MST}}{L_{GT} - L_{MST}}, \quad (4)$$

where L_{EXP} , L_{MST} and L_{GT} correspond respectively to the total length of the network in the experiment, the corresponding minimal spanning tree and the greedy triangulation. Accordingly, we calculate a normalized $E_{glob,G}^*$ and f_R^* between the MST and the GT defined respectively as:

$$E_{glob,G}^* = \frac{E_{glob,G}^{EXP} - E_{glob,G}^{MST}}{E_{glob,G}^{GT} - E_{glob,G}^{MST}} \quad (5)$$

and

$$f_R^* = \frac{f_R^{EXP} - f_R^{MST}}{f_R^{GT} - f_R^{MST}}. \quad (6)$$

Network cost varies from values close to the MST cost (minimal observed $c = 0.067$) to values that did not exceed half the triangulation cost (maximal observed $c = 0.410$). However, as E_{glob}^* and f_R^* increase faster than the cost (Fig. 5), high level of path system efficiency and robustness can be reached with a slight increase in cost.

6 Discussion

Ant networks of galleries provide a well-defined example of a self-organized graph resulting from a set of parallel distributed decisions made by a set of simple agents. The problem considered here is relevant in a number of ways. The first is its planar character, not shared by other previously analyzed graphs embedded on two-dimensional domains [41,42]. The second major difference arises from the dynamics of its evolution. Instead of having a dynamics based on multiplicative processes (such as preferential attachment) or top-down (global) optimization, a spatially localized set of interactions among ants and the gallery structure leads to a final, stationary graph with well-defined properties. The key results obtained from our study can be summarized as follows:

(1) The gallery networks display a single-scale, exponential degree distributed. Such distribution is largely constrained by the spatial constraints imposed by the two-dimensional setting.

(2) In the largest networks, the characteristics of the path system and their fragmentation under node removal are closer to the one of a triangulated network though their cost is closer to the one a tree.

(3) These networks exhibit resilience to random disconnections but vulnerability to the preferential removal of high-degree vertices, while classical random graphs exhibit no difference in their robustness to these different processes of disconnection. The origin of these properties were thus first considered as unique features of the scale-free networks. However, it was also observed in food-webs with single-scaled degree distributions, and our results suggest further that it may be linked with a more generic characteristic of real networks that may be the asymmetric nature of their link patterning [39]. Indeed, we have observed that robustness increased with the skewedness of the degree distribution.

(4) Efficiency is reached by increasing the meshedness, that is, in the networks of galleries, by merging trees. Such spatial patterning might be related to evolutionary pressures (see below).

(5) The origin of these similarities with triangulated networks may rely in the structure of cycles. When the network size increases, tree structures rapidly lose much efficiency and robustness. However, the introduction of a small amount of cycles, as our results suggested, may be sufficient to suppress or slow down size effects. In this study, we have introduced a meshedness coefficient based on the Euler relation. It is easy to compute, but it is not possible to generalize this measure to non-planar networks. The importance of the structure of cycles has been recently suggested as a possible major trait of the topological organization of complex networks [23,43,44]. A key issue will consist in developing generic methods addressing this question in networks regardless of their nature, and to determine if there exist common properties in the structure of cycles in different real world networks.

In underground ant [17,45] and termite nests [46], or in the burrowing system of rodents such as mole-rats [47,48], networks of galleries evolved from simple trees to mesh

networks. This increase in the nest complexity is generally correlated with the increase of the nest size and the number of individuals in the colony [17,45,46]. Since these networks are the topological scenario where the life of the colony takes place, large nests with thousands or even millions of individuals are likely to display some invariant adaptive properties in their topology. Paradoxically, the absence of methods to characterize complex networks has long resulted in considering the large networks of galleries as amorphous structures lacking any apparent regularities in comparison with above ground nests [17,21,49]. As we have shown, complex network methods may reveal some invariant properties of these nests and open an insight about functional aspects of their topology in terms of robustness, displacements and communication efficiency. Future work should explore the possibility of an optimization process under a number of constraints and how the interplay of efficiency, robustness and cost might have shaped their structure.

The authors would like to thank V. Fourcassié, C. Jost and R. Bon for many helpful suggestions and comments. J. Buhl was supported by a doctoral grant from the French Ministry of Scientific Research. J.L. Deneubourg is a research associate of the Belgian National Foundation for Scientific Research. This work has been supported by the "Programme Cognitique" from the French Ministry of Scientific Research (JB, JG, GT), by the grant BFM2001-2154 (RVS, SV) and the Santa Fe Institute (RVS).

References

1. R. Albert, A.L. Barabasi, *Rev. Mod. Phys.* **74**, 47 (2002)
2. S. Bornholdt, H.G. Schuster, *Handbook of Graphs and Networks: from the genome to the internet* (Wiley-VCH, Berlin, 2003)
3. M.E.J. Newman, *Siam Rev.* **45**, 167 (2003)
4. D.J. Watts, *Small Worlds: The Dynamics of Networks Between Order and Randomness* (Princeton University Press, Princeton, 1999)
5. L.A.N. Amaral, A. Scala, M. Barthelemy et al., *Proc. Natl. Acad. Sci. USA* **97**, 11149 (2000)
6. R.V. Solé, R. Ferrer i Cancho, J.M. Montoya et al., *Complexity* **8**, 20 (2002)
7. R. Ferrer i Cancho, C. Janssen, R. Solé, *Phys. Rev. E* **64**, 046119 (2001)
8. E. Schaur, *Non-planned Settlements* (Institute for Lightweight Structures, Stuttgart, 1992)
9. D. Helbing, F. Schweitzer, J. Keltsch et al., *Phys. Rev. E* **56**, 2527 (1997)
10. K.N. Ganeshaiah, T. Veena, *Behav. Ecol. Sociobiol.* **29**, 263 (1991)
11. F. Lopez, F.J. Acosta, J.M. Serrano, *J. Anim. Ecol.* **63**, 127 (1994)
12. G. Délye, *Insect. Soc.* **18**, 15 (1971)
13. G. Thomé, *Insect. Soc.* **19**, 95 (1972)
14. M. Brian, *Social insects: Ecology and Behavioural Biology* (Chapman and Hall, London, 1983)
15. P. Cerdan, Ph.D. thesis, Université de Provence, Aix-Marseille I, 1989
16. P. Rasse, Ph.D. thesis, Université Libre de Bruxelles, Brussels, 1999
17. D. Cassill, W.R. Tschinkel, S.B. Vinson, *Insect. Soc.* **49**, 158 (2002)
18. W.R. Tschinkel, *Insect. Soc.* **34**, 143 (1987)
19. W.R. Tschinkel, *Ecol. Entomol.* **24**, 222 (1999)
20. A.S. Mikheyev, W.R. Tschinkel, *Insect. Soc.* **41**, 30 (2004)
21. W.R. Tschinkel, *Palaeogeogr. Palaeoclimatol. Palaeoecol.* **192**, 321 (2003)
22. T. Nishizeki, N. Chiba, *Planar Graphs; Theory and Algorithms* (North-Holland, Amsterdam, 1988)
23. G. Caldarelli, R. Pastor-Satorras, A. Vespignani, *Eur. Phys. J. B* **38**, 183 (2004)
24. B. Bollobas, *Random graphs*, 2nd edn. (Cambridge University Press, Cambridge, 2002)
25. A. Denise, M. Vasconcellos, D.J.A. Welsh, *Congressus Numerantium* **113**, 61 (1996)
26. D. Osthus, H.J. Promel, A. Taraz, *J. Comb. Theory B* **88**, 119 (2003)
27. I. Rodriguez-Iturbe, A. Rinaldo, *Fractal river basins: chance and self-organization* (Cambridge University Press, Cambridge, 1997)
28. E.W. Dijkstra, *Numer. Math.* **1**, 269 (1959)
29. J.B. Kruskal, *Proc. Amer. Math. Soc.* **2**, 48 (1956)
30. D. Cheriton, R.E. Tarjan, *SIAM J. Computing* **5**, 724 (1976)
31. M. de Berg, M. van Kreveld, M. Overmars et al., *Computational geometry*, 2nd rev. edn. (Springer, Berlin, 2000)
32. M. Garey, D. Johnson, *Computers and intractability, a guide to the theory of NP-Completeness* (W.H. Freeman, New York, 1979)
33. C. Levkopoulos, A. Lingas, *Algorithmica* **2** (1987)
34. V. Latora, M. Marchiori, *Eur. Phys. J. B* **32**, 249 (2003)
35. R. Albert, H. Jeong, A.L. Barabasi, *Nature* **406**, 378 (2000)
36. P. Holme, B.J. Kim, C.N. Yoon et al., *Phys. Rev. E* **65**, 056109 (2002)
37. H. Jeong, S.P. Mason, A.L. Barabasi et al., *Nature* **411**, 41 (2001)
38. R.V. Solé, J.M. Montoya, *Proc. R. Soc. Lond. B Biol. Sci.* **268**, 2039 (2001)
39. J.A. Dunne, R.J. Williams, N.D. Martinez, *Ecol. Lett.* **5**, 558 (2002)
40. M.E.J. Newman, *Phys. Rev. Lett.* **89**, 208701 (2002)
41. M. Kaiser, C.C. Hilgetag, *Phys. Rev. E* **69**, 036103 (2004)
42. S.S. Manna, A. Kabakçiuglu, *J. Phys. A* **36**, L279 (2003)
43. G. Bianconi, *Eur. Phys. J. B* **38**, 223 (2004)
44. D. Garlaschelli, *Eur. Phys. J. B* **38**, 277 (2004)
45. B. Hölldobler, E.O. Wilson, *The ants* (Springer, Berlin Heidelberg, New York, 1990)
46. P.P. Grassé, *Termitologia*, Tome II, *Fondation des Sociétés. Construction* (Masson, Paris, 1984)
47. K.C. Davies, J.U.M. Jarvis, *J. Zool. Lond.* **209**, 125 (1986)
48. S.C. Le Comber, A.C. Spinks, N.C. Bennett et al., *Can. J. Zool.* **80**, 436 (2002)
49. A. Forel, *Neue Denkschr. Allg. Schweiz. Ges. Gesamten Naturwiss.* **26**, 1 (1874)